White Rose Research Online

eprints@whiterose.ac.uk
https://eprints.whiterose.ac.uk
Universities of Leeds, Sheffield and York

Deposited via The University of Sheffield.

White Rose Research Online URL for this paper:
https://eprints.whiterose.ac.uk/id/eprint/241200/

Version: Published Version

**Article:**
Jin, X., Yi, X., Ng, B.K. et al. (2026) A model to determine multiplication and noise in avalanche photodiodes with non-uniform electric field. AIP Advances, 16 (5). 055114. ISSN: 2158-3226

https://doi.org/10.1063/5.0326874

**Reuse**
This article is distributed under the terms of the Creative Commons Attribution (CC BY) licence. This licence allows you to distribute, remix, tweak, and build upon the work, even commercially, as long as you credit the authors for the original work. More information and the full terms of the licence here: https://creativecommons.org/licenses/

**Takedown**
If you consider content in White Rose Research Online to be in breach of UK law, please notify us by emailing eprints@whiterose.ac.uk including the URL of the record and the reason for the withdrawal request.

AIP Advances

RESEARCH ARTICLE | MAY 13 2026

# A model to determine multiplication and noise in avalanche photodiodes with non-uniform electric field

Xiao Jin ; Xin Yi ; Beng Koon Ng ; Chee Hing Tan ; Duu sheng Ong ; John P. R. David

*AIP Advances* 16, 055114 (2026)
https://doi.org/10.1063/5.0326874

**Articles You May Be Interested In**

Driven by Brownian motion Cox–Ingersoll–Ross and squared Bessel processes: Interaction and phase transition

*Physics of Fluids* (January 2025)

The new effect of oscillations of the total angular momentum vector of viscous fluid

*Physics of Fluids* (August 2022)

18 May 2026 15:41:39

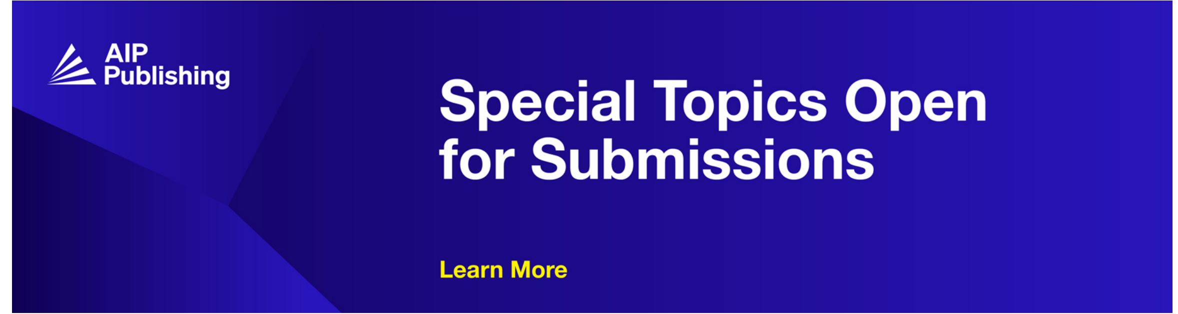

# A model to determine multiplication and noise in avalanche photodiodes with non-uniform electric field

Cite as: AIP Advances 16, 055114 (2026); doi: 10.1063/5.0326874
Submitted: 11 February 2026 • Accepted: 29 April 2026 •
Published Online: 13 May 2026

View Online

Export Citation

CrossMark

Xiao Jin,[1,a)] Xin Yi,[2] Beng Koon Ng,[3] Chee Hing Tan,[1] Duu sheng Ong,[4] and John P. R. David[1,a)]

## AFFILIATIONS

[1] Department of Electronic and Electrical Engineering, University of Sheffield, Sheffield S1 3JD, United Kingdom
[2] Institute of Photonics and Quantum Sciences, School of Engineering and Physical Sciences, Heriot-Watt University, David Brewster Building, Edinburgh EH14 4AS, United Kingdom
[3] Scool of Electrical & Electronic Engineering, Nanyang Technological University, Singapore 639798, Singapore
[4] Faculty of Artificial Intelligence and Engineering, Multimedia University, 63100 Cyberjaya, Selangor, Malaysia

[a)] **Authors to whom correspondence should be addressed:** xjin4@outlook.com and j.p.david@sheffield.ac.uk

## ABSTRACT

A modification to the random path length technique (RPL) with a hard-threshold dead space ($E_{th}$) is demonstrated to be able to calculate the electron initiated avalanche multiplication ($M_e$) and excess noise ($F_e$) in GaAs $p^+$–$i$–$n^+$ structures with $n$- and $p$-type background doping levels up to $1 \times 10^{17}$ cm$^{-3}$ in the multiplication region. This model's $M_e$, $F_e$, and position dependent ionization probabilities are compared with the results obtained from a multi-valley analytical band Monte Carlo model, enabling us to quantify how the ionization process is affected when the electric field changes rapidly. The RPL results for $M_e$ show excellent agreement with the Monte Carlo model, suggesting that the simple hard dead-space correction to the ionization probability distribution function works as well with a varying electric field up to 1400 kV/cm/$\mu$m as in a constant electric field and that the "history dependence" effects of a varying electric field are not very significant once the initial carrier dead space is allowed for. The modified RPL $F_e$ also agrees well with the Monte Carlo model for $p^+$–$n^-$–$n^+$ structures; however, it is underestimated for $p^+$–$p^-$–$n^+$ structures. This is attributed to the hard dead space of the feedback carriers having a disproportionate effect on the variance in the multiplication.

© *2026 Author(s). All article content, except where otherwise noted, is licensed under a Creative Commons Attribution (CC BY) license (https://creativecommons.org/licenses/by/4.0/).* https://doi.org/10.1063/5.0326874

18 May 2026 15:41:39

## I. INTRODUCTION

An accurate determination of the performance of avalanche photodiodes requires knowledge of the mean multiplication, $\langle M \rangle$, for the gain and $\frac{\langle M^2 \rangle}{\langle M \rangle^2}$ for the excess noise, $F$. The determination of the multiplication, $M$, in turn requires knowledge of the electron ($\alpha$) and hole ($\beta$) ionization coefficients, which are usually defined as functions of the electric field. It is well known that carriers need to gain energy from the electric field before they can undergo impact ionization, and consequently, it is not always possible to simply attribute values of $\alpha$ and $\beta$ to the local electric field at a particular position in a structure.[1] There have been various attempts to account for this "dead-space" region, where no ionization occurs, in both analytical[2–6] and Monte Carlo based numerical models[7–10] used to determine $M$ and $F$ in APDs. The effect of this dead space on the ionization coefficients and, hence, multiplication is not very significant at low electric fields, where the mean distance between ionization events is large compared to the distance carriers travel to gain the ionization threshold energy ($E_{th}$).[4,11] At high electric fields, the mean ionization distance decreases almost exponentially and starts to approach the dead space distance,[12] so in thin avalanching structures, the dead-space results in a suppression of the multiplication[13,14] and, more importantly for avalanche photodiodes (APDs), a reduction in their excess noise.[15] The conventional excess noise model by McIntyre[16] assumes that the electron and hole ionization probability distribution functions (PDFs) are perfect exponential functions, and this gives rise to the relationship relating the $F$ to the $\boldsymbol{\beta}/\boldsymbol{\alpha}$ ratio. The presence of dead-space, however, results in

displaced exponential PDFs that no longer follow the usual McIntyre expression. Hayat *et al.*[4] came up with a technique using coupled integral equations that allowed the incorporation of a dead space into the ionization PDF to calculate the $M$ and $F$. Ong *et al.*[17] came up with an alternative way of incorporating the dead space while solving these equations numerically using randomly generated ionization path lengths that gave essentially identical results. The $M$ and $F$ are calculated using this Random Path Length (RPL) technique from the average of many individual multiplication trials (>50 000). These techniques have been used successfully to model the behavior of different thickness $p$–$i$–$n$ and $n$–$i$–$p$ diodes down to 50 nm;[17] however, they have hitherto been limited to structures where the electric field in the multiplication region is constant. In many real devices, the presence of even modest unintentional doping in the high field multiplication region results in a varying electric field, such that, in addition to the dead space, there may be issues related to the "history dependence" of the ionization process due to the electric field gradient.[6] Quade *et al.*[18] showed from hydrodynamic modeling that the ionization coefficients in heavily doped p–n junctions are different from those given by the local electric field. Hydrodynamic and energy-balance models,[19] however, require knowledge of the carrier temperature or energy and are, therefore, difficult to use. Plimmer *et al.*[20] and Mun *et al.*[21] investigated the effect of a varying electric field on $M$ and $F$ using a simple Monte Carlo (SMC) model where only one conduction and one valence band were used. This SMC model, however, does not capture the true high field behavior of carriers and is also relatively complicated to use. McIntyre suggested in 1999[16] that when the electric field varies with distance, the local electric field at a particular position may not represent the carrier ionization behavior, and the history dependence of its previous trajectory needs to be considered. This "history" dependent model was used successfully to replicate the $M$ and $F$ behavior in thin structures but only with a constant electric field by Yuan *et al.*[22]

In this work, we explain how the RPL model can be modified to enable it to simulate the impact ionization process in a varying electric field while still incorporating a hard dead space. Furthermore, we compare $M_e$ and $F_e$ in GaAs $p$–$i$–$n$ diodes with different levels of doping and, therefore, electric field gradients made with this modified RPL model (hereafter the MRPL model) with an experimentally benchmarked analytical band Monte Carlo model for GaAs. The results suggest that while $M_e$ between models agrees well for doping up to $1 \times \mathbf{10^{17}}$ cm$^{-3}$ in the multiplication region, as does $F_e$ for the $p^+$–$n^-$–$n^+$ structure, $F_e$ given by the MRPL for the $p^+$–$p^-$–$n^+$ is increasingly underestimated due to a lower feedback of carriers with a hard dead space.

The experimental ionization coefficients in GaAs covering a wide electric field range have been determined by Plimmer *et al.*,[23] and Ong *et al.*[12] used a three valley analytical band Monte Carlo model to fit to this experimental data. In doing this study, using a full band Monte Carlo model[24] would allow the physics of the ionization process in GaAs to be undertaken more accurately; however, this would be extremely time consuming. Simpler analytical band Monte Carlo models,[12] while faster and capable of replicating the mean ionization path lengths, would not capture the complex manner by which carriers gain or lose energy as they scatter between the different valleys and bands. This is especially true for electrons, where the ionization process occurs in the second (or higher) conduction band.[24] Consequently, we have used a modified analytical Monte Carlo model[25] (MAMC) to describe the electron ionization behavior. In this four-valley model, the first conduction band consists of three non-parabolic valleys, $\Gamma_6$, $L_6$, and $X_6$, while the second conduction band is approximated by a single valley representing that at $X_7$. A hard threshold energy of 6 eV is set for ionization in this band. This is capable of replicating the mean and the PDFs of electron impact ionization path length, energy, and time, as well as the transient drift velocity, at electric fields up to 900 kV/cm, in good agreement with full band MC models.[24] The hole transport was dealt with by having an analytical approximation of the first three valence bands, namely, heavy hole, light hole, and spin split-off bands. This model is capable of replicating the ionization behavior accurately for electric fields up to 700 kV/cm, as shown by a comparison with the experimental data of Plimmer *et al.*[23] in Fig. 1(a), while being computationally more efficient.

The ionization coefficients obtained from the MAMC have been parameterized into Chynoweth equations [Eqs. (1) and (2)] for $\alpha$ and $\beta$ and used as an input to the MRPL model to determine $M$ and $F$ as a function of electric field (ε),

$$\alpha = \begin{cases} 2.28 \times 10^5 \exp\left(-\left(\dfrac{6.77 \times 10^5}{\varepsilon}\right)^{1.511}\right)\text{cm}^{-1} \\ \text{when } \varepsilon < \dfrac{700\text{kV}}{\text{cm}}, \\ 2.18 \times 10^5 \exp\left(-\left(\dfrac{6.70 \times 10^5}{\varepsilon}\right)^{2.2}\right)\text{cm}^{-1} \\ \dfrac{\text{when } 700\text{kV}}{\text{cm}} < \varepsilon < 1000\dfrac{\text{kV}}{\text{cm}}, \end{cases} \tag{1}$$

$$\beta = \begin{cases} 2.24 \times 10^5 \exp\left(-\left(\dfrac{7.148 \times 10^5}{\varepsilon}\right)^{1.554}\right)\text{cm}^{-1} \\ \text{when } \varepsilon < \dfrac{700\text{kV}}{\text{cm}}, \\ 2.18 \times 10^5 \exp\left(-\left(\dfrac{6.948 \times 10^5}{\varepsilon}\right)^{2.3}\right)\text{cm}^{-1} \\ \dfrac{\text{when } 700\text{kV}}{\text{cm}} < \varepsilon < \dfrac{1000\text{kV}}{\text{cm}}. \end{cases} \tag{2}$$

For the purposes of this paper, we will consider a 1 $\mu$m thick $p^+$–$n(p)^-$–$n^+$ GaAs structure with different levels of $n(p)$-type doping and with the $p^+$ and $n^+$ cladding doping levels set to $1 \times 10^{19}$ cm$^{-3}$, as shown in Fig. 1(b), thereby avoiding complications due to ionization in the depletion region of the cladding layers. The original RPL model[17] was developed for the situation when the electric field was constant in the high field multiplication region, so the shape of the ionization PDF was identical irrespective of the starting position within this multiplication region. In the hard dead-space model, impact ionization can only occur after a carrier gains at least the ionization threshold energy ($E_{th}$). The probability for an electron to impact and ionize for the first time after traveling a distance $x$ in a constant electric field, $P_{e(x)}$, is given by Eq. (3) from Ref. 17 as

$$P_e(x) = \begin{cases} 0, x \leqslant d_e^*, \\ \alpha^* \exp\left[-\alpha^*\left(x - d_e^*\right)\right], x > d_{e,}^* \end{cases} \tag{3}$$

where $\alpha^*$ is the ionization probability per unit distance after the dead-space, given by[17]



© Author(s) 2026

18 May 2026 15:41:39

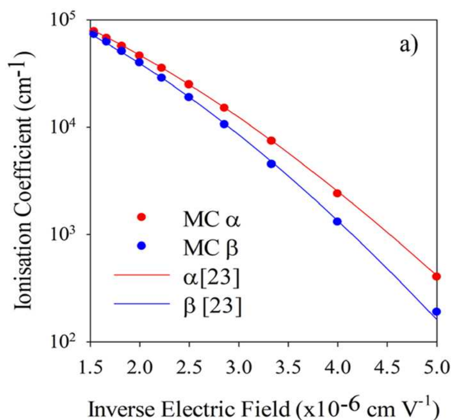


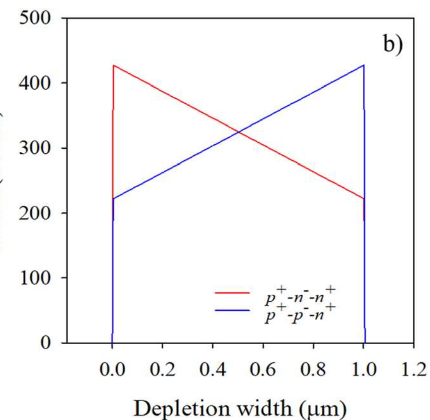


**FIG. 1.** (a) GaAs impact ionization coefficients for electrons (α) and holes (β) reported by Plimmer *et al.*[23] and compared with α and β from the modified analytical MC model. (b) A schematic diagram of the electric field profile in a 1 $\mu$m thick $p^+$–$i^-$–$n^+$ GaAs structure with $p^+$ and $n^+$ cladding doping levels set to 1 × $10^{19}$ $cm^{-3}$ and n(*p*) type doping of 1.5 × $10^{16}$ $cm^{-3}$.

$$\alpha = \frac{1}{d_e^* + 1/\alpha^*}, \tag{4a}$$

and the electron hard threshold dead-space, $d_e^*$, is given by

$$d_e^* = \frac{E_{\text{th}}^*}{q\mathcal{E}}, \tag{4b}$$

where $q$ is the electronic charge and $\mathcal{E}$ is the electric field.

From Eq. (3), the probability that a carrier has traveled a distance $x$ without producing an electron–hole pair (the survival probability) becomes

$$S_e(x) = \begin{cases} 1, x \leqslant d_e^*, \\ \exp\left[-\alpha^*\left(x - d_e^*\right)\right], x > d_e^*, \end{cases} \tag{5}$$

where $P_e(x)$ and $S_e(x)$ are shown in Figs. 2(a) and 2(b), respectively, by the dashed green lines. In Fig. 2 and subsequent diagrams, the $p^+$ region is assumed to be at the left of the figure with electrons injected at $x = 0$ $\mu$m.

The injected electron impact ionizes at position $x = l_e$, and a random electron ionization path length $l_e$ can be generated by substituting a uniformly distributed random number $r$ between 0 and 1 for $S_e(x)$ as

$$l_e = d_e^* - \frac{\ln\ (r)}{\alpha^*}. \tag{6}$$

Secondary carriers (one electron and one hole) are generated. A new random number will be generated independently for the original carrier and the two newly generated carriers to determine their respective ionization path lengths using Eq. (6). Electrons and holes continue to repeat this process independently, and the total number of ionization events within the multiplication region is recorded until the ionization process finishes. The multiplication is determined by taking the average of at least 50 000 trials.

These equations need to be modified when there is an electric field that varies with distance, and the ionization PDF has to change shape from a simple exponential in such a situation. We look at the case when the electron (hole) ionization threshold energies, $E_{the(h)}$ = 3 eV, are in the presence of a doped multiplication region. For the sake of simplicity and to demonstrate the concept, we assume a constant doping and, therefore, a linearly varying electric field in the

18 May 2026 15:41:39

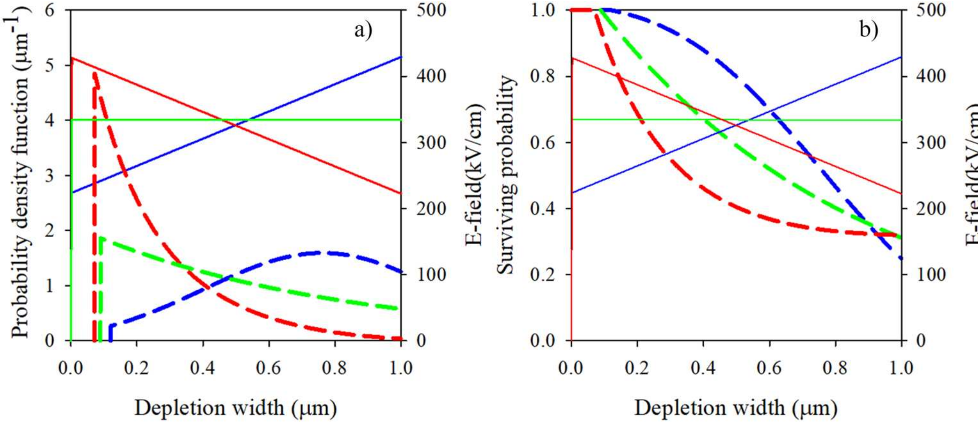


**FIG. 2.** (a) Probability density function (PDF) for electrons injected at $x = 0$ with $E_{th}$ = 3 eV (dashed lines) at $M_e \approx 10$: green for $p^+$–$i$–$n^+$, red for $p^+$–$n^-$–$n^+$, and blue for $p^+$–$p^-$–$n^+$. (b) Surviving probability for electrons injected at $x = 0$ with $E_{the}$ = 3 eV (dashed lines) at $M_e \approx 10$: green for $p^+$–$i$–$n^+$, blue for $p^+$–$p^-$–$n^+$, and red for $p^+$–$n^-$–$n^+$.


© Author(s) 2026

multiplication region. Still assuming a hard dead space, the electron dead space, $d_e^*$, is now given by

$$E_{th}\ (x) = q \cdot \int_{x_0}^{d_e^*} \mathcal{E}(x)dx. \tag{7}$$

The threshold energy is calculated by integrating the total amount of energy an electron acquires while traveling in the varying electric field. The dead space distance will be different for different starting positions, $x_0$, of the initiating carrier due to the varying electric field, whereas in previous cases, the electric field is constant across the multiplication region so that the dead space distance is also constant. Equation (1) now becomes

$$P_e(x) = \begin{cases} 0, x \leqslant d_e^*, \\ \alpha^*\left(x_0 + d_e^*\right) \cdot \exp^{-\int_{x_{0+d_e^*}}^{x} \alpha^*(x')\cdot dx'}, x > d_e^*, \end{cases} \tag{8}$$

where $\alpha^*$ is the ionization probability per unit distance after the dead space, and $\exp^{-\int_{x_{0+d_e^*}}^{x} \alpha^*(x')\cdot dx'}$, describes the probability of a carrier getting to this position without having previously ionized.

The survival probability ($S_e$) that a carrier has traveled a distance $x$ without producing an electron–hole pair becomes

$$S_e(x) = \begin{cases} 1, x \leqslant d_e^*, \\ 1 - \int_{x_{0+d_e^*}}^{x} P_e(x)dx, x > d_{e,}^* \end{cases} \tag{9}$$

$$S_e(x) = 1 - \int_{x_{0+d_e^*}}^{x} \alpha^*\left(x_0 + d_e^*\right) \cdot \exp^{-\int_{x_{0+d_e^*}}^{x} \alpha^*(x')\cdot dx'} dx, \tag{10}$$

$$S_e(x) = \exp^{-\int_{x_{0+d_e^*}}^{x} \alpha^*(x')\cdot dx'} \quad \text{for } x > d_e^*. \tag{11}$$

In this case, a random electron ionization path length, $l_e$, can be generated by substitution of a uniformly distributed random number $r$ between 0 and 1 for $S_e(x)$ in Eq. (11). Therefore,

$$S_e(x) = r \tag{12}$$

and

$$\Rightarrow \textstyle\sum_{x_{0+d_e^*}}^{x} \alpha(x)\Delta x = -\ln\ (r) \quad \text{for } x > d_e^*. \tag{13}$$

With a varying electric field profile, the mean ionization path length not only depends on the current position of a carrier but also on the subsequent electric field profile, as $\alpha$ changes with the electric field. Similar arguments apply for holes by substituting $P_h(x)$, $S_h(x)$, and $l_h$ in the equations above.

Having an $n$-type multiplication region doping level of $1.5 \times 10^{16}$ cm$^{-3}$ and with an applied bias of 31.37 V (corresponding to $M_e \approx 10$) results in a linearly decreasing electric field with distance [the solid red line in Fig. 2(a)], and the exponentially decaying PDF of an electron injected at $x = 0$ is modified to that shown by the dashed red line. Figure 2(b) shows the survival probability ($S_e$) of this electron injected at $x = 0$ traveling across the multiplication region without ionizing. Similarly, Figs. 2(a) and 2(b) also show the ionization PDF and survival probability $S_e$ of a carrier injected at $x = 0$ for a multiplication region with a $p$-doping level of $1.5 \times 10^{16}$ cm$^{-3}$, with a similar applied bias of 31.58 V ($M_e \approx 10$), which gives the opposite electric field gradient (the solid blue line). The electron ionization probability and the survival probability in this case appear very different from those of the $n$-type doping, as shown by the dashed blue lines in Figs. 2(a) and 2(b), respectively.

The ionization PDF and survival probability for carriers created at an arbitrary point in the multiplication region are simply calculated by using Eqs. (4)–(6) and (8) and replacing $x_0$ by their new starting position. Unlike in the case of a constant electric field in $p$–$i$–$n$'s, the shape of the ionization PDF and the survival probability will be different depending on the position from which the electron starts in the high field region. Using this technique, the MRPL model can be used to generate the mean multiplication and excess noise in $p^+$–$n(p)$–$n^+$ structures for multiplication due to electrons injected at $x = 0$. In order to test how well this MRPL model works with a rapidly varying electric field, we compare simulations of the multiplication and excess noise in $p^+$–$n(p)$–$n^+$ structures with different levels of doping (and therefore electric field gradients) obtained using the MAMC model.

## II. RESULT

Figures 3(a) and 3(c) show that $M_e$ from both models is similar for doping levels up to $1 \times 10^{17}$ cm$^{-3}$ in both $p^+$–$n^-$–$n^+$ and $p^+$–$p^-$–$n^+$ structures. Also shown by dashed lines is $M_e$ given by a purely local model simulation where dead space effects are ignored. It is clear that a local model increasingly overestimates $M_e$ and underestimates the breakdown voltage as the doping increases. Figure 3(b) shows that $F_e$ vs $M_e$ is also very similar between the MRPL and MAMC models for all the doping levels investigated in the $p^+$–$n^-$–$n^+$ structures. However, Fig. 3(d) shows that $F_e$ vs $M_e$ is underestimated by the MRPL model compared to the MAMC model for the $p^+$–$p^-$–$n^+$ model and that the difference increases with increasing doping. $F_e$ given by the local model and shown by the colored dashed lines in Figs. 3(b) and 3(d) is overestimated due to ignoring any dead space effects and is simply given by the $\beta/\alpha$ ratio.[16]

In order to better understand the reason for the results shown in Fig. 3, a series of $p^+$–$n^-$–$n^+$ and $p^+$–$p^-$–$n^+$ structures were simulated with $n$-type ($p$-type) doping levels of $1.5 \times 10^{16}$, $5 \times 10^{16}$, and $1 \times 10^{17}$ cm$^{-3}$. Electrons were injected at $x = 0$ $\mu$m for applied voltages and their corresponding electric field profiles [shown by the dark green solid lines in Figs. 4(a)–4(f)] that would give $M_e$ ~10 with the MRPL. Note that at the higher doping levels, the doped 1 $\mu$m multiplication layer is not necessarily fully depleted. For each injected electron, the position where all electrons and holes ionize for these electric field profiles is logged, and the average of 50 000 trials is undertaken in the MRPL model and 200 000 trials for the MAMC model. From these, a normalized position dependent ionization probability density (IPD) in the devices can be obtained for electrons (dotted red line) and holes (dotted blue line),

18 May 2026 15:41:39


© Author(s) 2026

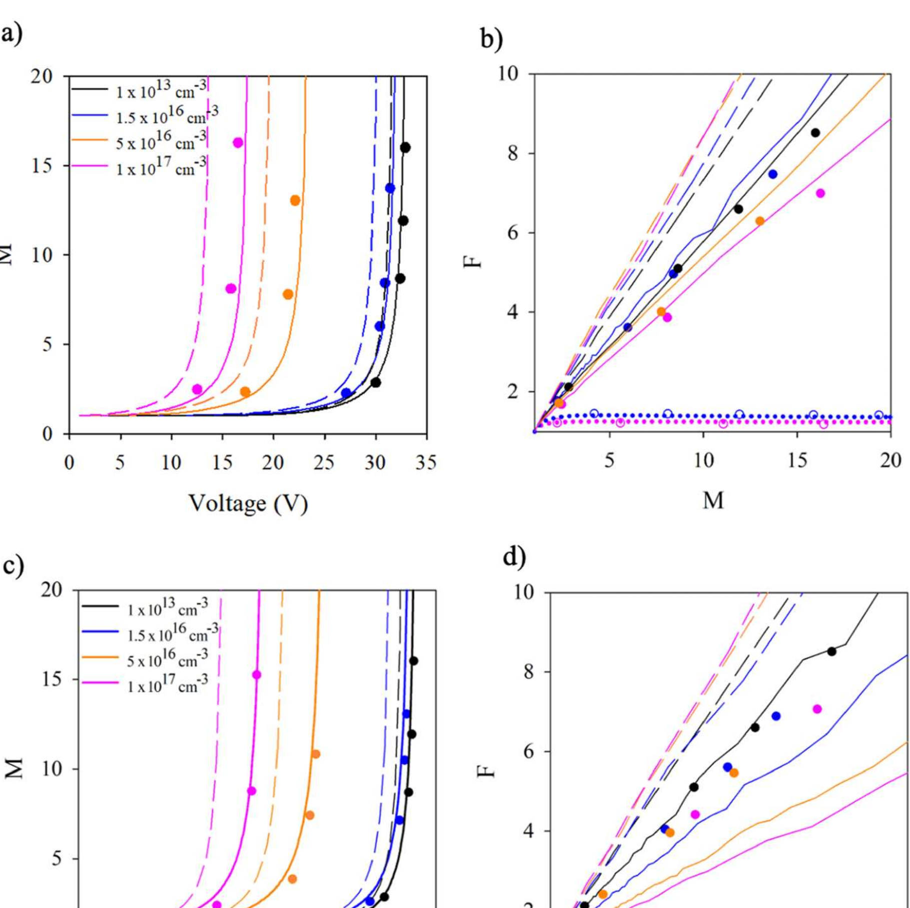


**FIG. 3.** A comparison of (a) multiplication and (b) excess noise between MRPL and Monte Carlo models for $p^+$–$n^-$–$n^+$ structures. A similar comparison between (c) multiplication and (d) excess noise between MRPL and Monte Carlo models for $p^+$–$p^-$–$n^+$ structures. Solid lines are MRPL results, and symbols are MAMC for $\beta \neq 0$. In panels (b) and (d), the dotted lines are MRPL $F_e$ results, and open symbols are MAMC $F_e$ results for $\beta = 0$. The dashed lines are MRPL results when $E_{the(h)} = 0$ eV and $\beta \neq 0$.

18 May 2026 15:41:39

as shown in Figs. 4(a)–4(f). We define this IDP as the total number of electron-initiated ionization events at position $x$ divided by the total number of electron-initiated ionization events for $M_e \approx 10$. A similar simulation was then done with the MAMC model, and Fig. 4 also shows the normalized position dependent IPD for electrons (red solid lines) and holes (blue solid lines). The MAMC model is capable of dealing with non-equilibrium transport and so would be expected to replicate the spatial ionization behavior of electrons and holes accurately, even when the electric field changes rapidly with distance. Figure 4 shows that these normalized IPDs are very similar between the MRPL and MAMC models for the relatively low doped $p^+$–$n(p)$–$n^+$ structures with a doping of $1.5 \times 10^{16}$ cm$^{-3}$, but differences, which get progressively larger, start to appear as the doping increases. For the $1 \times 10^{17}$ cm$^{-3}$ doped $p^+$–$n$–$n^+$ structure shown in Fig. 4(c), we can see that the electron IPD from the MRPL (red dotted line) peaks earlier and terminates earlier than that from the MAMC. This is attributed to the hard threshold dead space assumption in the MRPL model. Not only do the electrons starting at $x = 0$ have an initial dead space, but electrons created at or beyond ~0.38 $\mu$m also cannot gain $E_{the}$ from the electric field to initiate any further impact ionization. The electron IPD from the MAMC model (red solid line) has a lower peak value, which is displaced slightly further along, but the soft threshold energy implicit in the model allows electrons to ionize close to the far end of the depletion region, even when the electric field is low. The hole IPDs (blue dotted and solid lines) are qualitatively similar between the models. Despite these differences in the electron IPD, both $M_e$ and $F_e$ are similar between the models, as shown in Fig. 3. For the $p^+$–$p^-$–$n^+$ structure with $1 \times 10^{17}$ cm$^{-3}$ doping shown in Fig. 4(f), the biggest difference between the models is in the hole IPD. For electrons injected at $x = 0$ $\mu$m, holes are unable to ionize between 0.47 and 0.52 $\mu$m in the MRPL compared to the MAMC, where holes are ionizing much closer to the far depletion edge. Furthermore, holes in the MRPL also cannot ionize between 0 and 0.15 $\mu$m, as they cannot gain $E_{thh}$ in the low electric field region compared to holes created in the MAMC model. This overestimation of the dead space for feedback holes is responsible


© Author(s) 2026

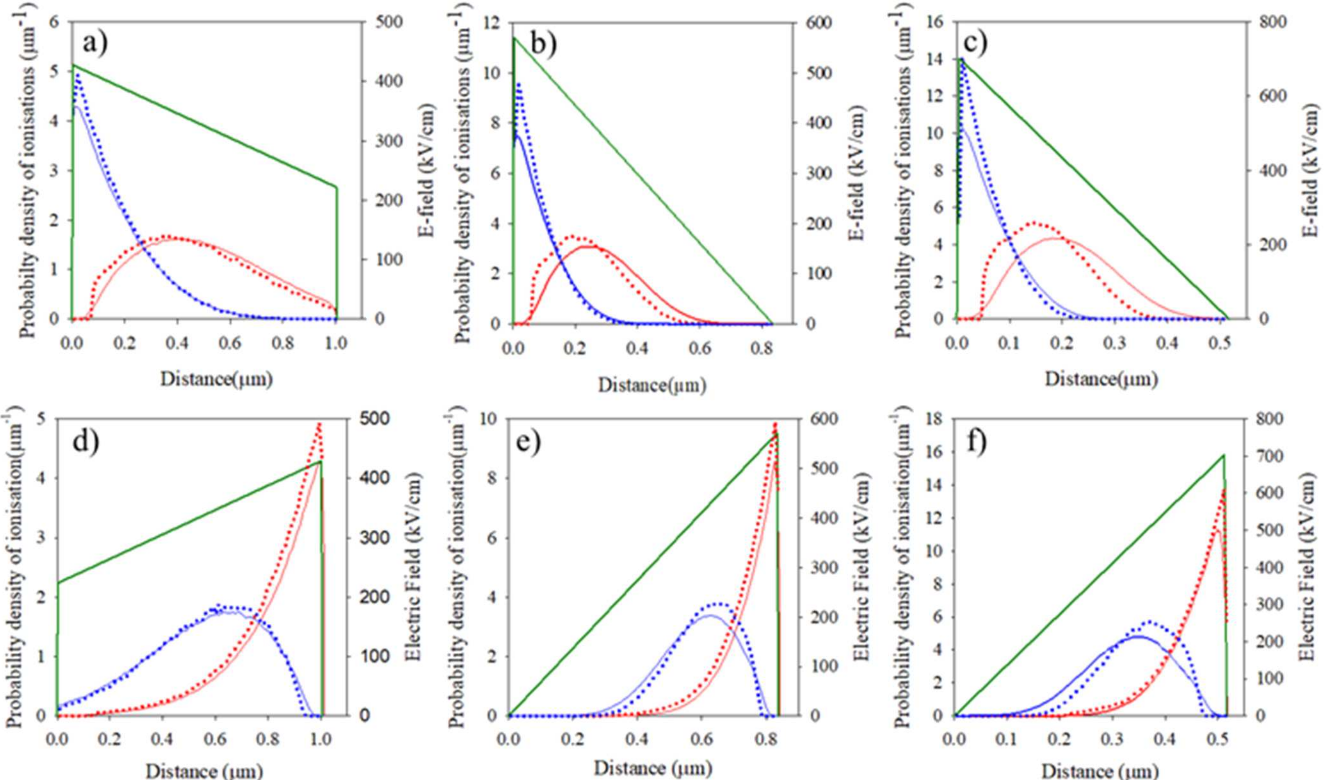


**FIG. 4.** Probability density of ionizations at different positions for electrons injected at $x = 0$ with $E_{the} = 3$ eV and $E_{thh} = 3$ eV at different $n$ type doping levels of (a) $1.5 \times 10^{16}$, (b) $5 \times 10^{16}$, and (c) $1 \times 10^{17}$ and different $p$ type doping levels of (d) $1.5 \times 10^{16}$, (e) $5 \times 10^{16}$, and (f) $1 \times 10^{17}$. The green solid lines are electric fields for $M \sim 10$ from MRPL. Red and blue dotted (solid) lines are MRPL (MAMC) results for electrons and holes, respectively.

18 May 2026 15:41:39

for the reduction in excess noise seen. The excess noise in APDs depends on the variance in $M$ and depends critically on the variance in how the feedback carrier ionizes. The feedback by holes in the $p^+–p^-–n^+$ MRPL case is constrained to the central part of the structure, and this directly reduces the variance in the $M$ that we will obtain, consequently reducing $F$. As the doping increases, the dead-space region at either end of the depletion region becomes more important for the feedback carrier and so reduces the excess noise. To confirm this, the hole ionization was set to zero in both models, and the new results of $F$ are also shown in Figs. 3(b) and 3(d) for the $1.5 \times 10^{16}$ and $1 \times 10^{17}$ cm$^{-3}$ doped cases. $F$ is $< 2$ due to $\beta = 0$ and the dead space effect, but the results are much more similar once we remove the variance in $M$ from feedback carriers between the models.

The hard threshold MRPL will have this limitation with feedback carriers ionizing more deterministically in $p^+–p^-–n^+$ structures, especially as both carrier types have similar ionization coefficients in GaAs. This effect would become less important for $M_e$ and $F_e$ in small $\beta/\alpha$ materials such as silicon[26] or recently reported Sb based alloys.[11,27–29] The incorporation of a soft threshold energy into the MRPL model would improve the determination of $F_e$ in $p^+–p^-–n^+$ structures but at the expense of some increased complexity in the model.

## III. CONCLUSION

A modification to the random path length technique (MRPL) incorporating a hard-threshold dead-space energy is demonstrated to be able to calculate the electron-initiated avalanche multiplication factor ($M_e$) and the corresponding excess noise factor ($F_e$) in GaAs $p^+–i–n^+$ structures even when the intrinsic doping level is as high as $1 \times 10^{17}$ cm$^{-3}$ within the multiplication region. By comparing the results with a multi-valley analytic band Monte Carlo model, we show that good agreement is obtained for $M_e$ with both $n$-type and $p$-type background doping; however, $F_e$ given by the MRPL for $p^+–p^-–n^+$ is underestimated due to the lower feedback of holes with a hard dead space.

## ACKNOWLEDGMENTS

The authors would like to thank the support from the Engineering and Physical Sciences Research Council (Grant Nos. EP/Y020855/1 and EP/W028166/1).

## AUTHOR DECLARATIONS

### Conflict of Interest

The authors have no conflicts to disclose.


© Author(s) 2026

## Author Contributions

All authors contributed equally to this work.

**Xiao Jin**: Conceptualization (lead); Formal analysis (lead); Methodology (lead); Writing – original draft (lead). **Xin Yi**: Data curation (supporting); Formal analysis (supporting). **Beng Koon Ng**: Data curation (supporting); Formal analysis (supporting). **Chee Hing Tan**: Data curation (supporting); Formal analysis (supporting). **Duu sheng Ong**: Conceptualization (equal); Data curation (lead); Supervision (lead). **John P. R. David**: Project administration (lead); Supervision (lead); Writing – review & editing (lead).

## DATA AVAILABILITY

The data that support the findings of this study are available from the corresponding authors upon reasonable request.

## REFERENCES


[1] Y. Okuto and C. R. Crowell, "Ionization coefficients in semiconductors: A nonlocalized property," Phys. Rev. B **10**(10), 4284–4296 (1974).
[2] K. M. van Vliet, A. Friedmann, and L. M. Rucker, "Theory of carrier multiplication and noise in avalanche devices—Part II: Two-carrier processes," IEEE Trans. Electron Devices **26**(5), 752–764 (1979).
[3] J. S. Marsland, "On the effect of ionization dead spaces on avalanche multiplication and noise for uniform electric fields," J. Appl. Phys. **67**(4), 1929–1933 (1990).
[4] M. M. Hayat, W. L. Sargeant, and B. E. A. Saleh, "Effect of dead space on gain and noise in Si and GaAs avalanche photodiodes," IEEE J. Quantum Electron. **28**(5), 1360–1365 (1992).
[5] A. Spinelli, A. Pacelli, and A. L. Lacaita, "Dead space approximation for impact ionization in silicon," Appl. Phys. Lett. **69**(24), 3707–3709 (1996).
[6] R. J. Mclntyre, "A new look at impact lonization-part I: A theory of gain, noise, breakdown probability, and frequency response," IEEE Trans. Electron Devices **46**(8), 1623–1631 (1999).
[7] H. Shichijo and K. Hess, "Band-structure-dependent transport and impact ionization in GaAs," Phys. Rev. B **23**(8), 4197–4207 (1981).
[8] K. Brennan, "Calculated electron and hold spatial ionization profiles in bulk GaAs and superlattice avalanche photodiodes," IEEE J. Quantum Electron. **24**(10), 2001–2006 (1988).
[9] J. Bude and K. Hess, "Thresholds of impact ionization in semiconductors," J. Appl. Phys. **72**(8), 3554–3561 (1992).
[10] G. M. Dunn, G. J. Rees, J. P. R. David, S. A. Plimmer, and D. C. Herbert, "Monte Carlo simulation of impact ionization and current multiplication in short GaAs diodes," Semicond. Sci. Technol. **12**(1), 111 (1997).
[11] B. Guo *et al.*, "Impact ionization coefficients of digital alloy and random alloy $Al_{0.85}Ga_{0.15}As_{0.56}Sb_{0.44}$ in a wide electric field range," J. Lightwave Technol. **40**(14), 4758–4764 (2022).
[12] D. S. Ong, K. F. Li, G. J. Rees, G. M. Dunn, J. P. R. David, and P. N. Robson, "A Monte Carlo investigation of multiplication noise in thin $p^+$-i-$n^+$ GaAs avalanche photodiodes," IEEE Trans. Electron Devices **45**(8), 1804–1810 (1998).
[13] S. A. Plimmer, J. P. R. David, and D. S. Ong, "The merits and limitations of local impact ionization theory," IEEE Trans. Electron Devices **47**(5), 1080–1088 (2000).
[14] S. A. Plimmer *et al.*, "Investigation of impact ionization in thin GaAs diodes," IEEE Trans. Electron Devices **43**(7), 1066–1072 (1996).
[15] M. C. Teich and B. E. A. Saleh, "Effect of dead space on gain and noise of double-carrier-multiplication avalanche photodiodes," IEEE Trans. Electron Devices **39**(3), 546–552 (1992).
[16] R. J. McIntyre, "Multiplication noise in uniform avalanche diodes," IEEE Trans. Electron Devices **ED-13**(1), 164–168 (1966).
[17] D. S. Ong, K. F. Li, G. J. Rees, J. P. R. David, and P. N. Robson, "A simple model to determine multiplication and noise in avalanche photodiodes," J. Appl. Phys. **83**(6), 3426–3428 (1998).
[18] W. Quade, M. Rudan, and E. Scho, "Hydrodynamic simulation of impact-ionization effects in P-N junctions," in *IEEE Transactions on Computer-Aided Design of Integrated Circuits and Systems* (IEEE, 1991), Vol. I.
[19] T. Grasser, T. Tang, H. Kosina, and S. Selberherr, "A review of hydrodynamic and energy-transport models for semiconductor device simulation," Proc. IEEE **91**(2), 251 (2003).
[20] S. A. Plimmer, C. H. Tan, J. P. R. David, R. Grey, K. F. Li, and G. J. Rees, "The effect of an electric-field gradient on avalanche noise," Appl. Phys. Lett. **75**(19), 2963–2965 (1999).
[21] S. C. L. T. Mun, C. H. Tan, Y. L. Goh, A. R. J. Marshall, and J. P. R. David, "Modeling of avalanche multiplication and excess noise factor in $In_{0.52}Al_{0.48}As$ avalanche photodiodes using a simple Monte Carlo model," J. Appl. Phys. **104**(1), 013114 (2008).
[22] P. Yuan *et al.*, "A new look at impact ionization-Part II: Gain and noise in short avalanche photodiodes," IEEE Trans. Electron Devices **46**(8), 1632–1639 (1999).
[23] S. A. Plimmer, J. P. R. David, G. J. Rees, and P. N. Robson, "Ionization coefficients in $Al_xGa_{1-x}As$ ($x$ = 0–0.60)," Semicond. Sci. Technol. **15**(7), 692 (2000).
[24] D. S. Ong, K. F. Li, S. A. Plimmer, G. J. Rees, J. P. R. David, and P. N. Robson, "Full band Monte Carlo modeling of impact ionization, avalanche multiplication, and noise in submicron GaAs $p^+$-i-$n^+$ diodes," J. Appl. Phys. **87**(11), 7885–7891 (2000).
[25] K. Y. Choo and D. S. Ong, "Analytical band Monte Carlo simulation of electron impact ionization in $In_{0.53}Ga_{0.47}As$," J. Appl. Phys. **96**(10), 5649–5653 (2004).
[26] R. Van Overstraeten, H. De Man, and H. D. E. Man, "Measurement of the ionization rates in diffused silicon p-n junctions," Solid. State. Electron. **13**(6), 583–608 (1970).
[27] X. Yi *et al.*, "Demonstration of large ionization coefficient ratio in $AlAs_{0.56}Sb_{0.44}$ lattice matched to InP," Sci. Rep. **8**(1), 9107 (2018).
[28] Y. Yuan, J. Zheng, A. K. Rockwell, S. D. March, S. R. Bank, and J. C. Campbell, "AlInAsSb impact ionization coefficients," IEEE Photonics Technol. Lett. **31**(4), 315–318 (2019).
[29] X. Jin *et al.*, "Very low excess noise $Al_{0.75}Ga_{0.25}As_{0.56}Sb_{0.44}$ avalanche photodiode," Opt. Express **31**(20), 33141–33149 (2023).


18 May 2026 15:41:39


© Author(s) 2026